

Femur Mass in a 43-Year-Old Woman

Yan Epelboym MPH, Kapil R. Desai MD,
Roberto Garcia MD, James C. Wittig MD

Received: 29 July 2011 / Accepted: 2 April 2012 / Published online: 12 May 2012
© The Association of Bone and Joint Surgeons® 2012

History and Physical Examination

A 43-year-old woman was seen in consultation for a lesion in her left distal femur. One year earlier she began experiencing pain in her left knee after a fall. The pain was worse at night and awakened the patient from sleep. The patient had a 26-year smoking history. Her family history

Each author certifies that he or she, or a member of their immediate family, has no commercial associations (eg, consultancies, stock ownership, equity interest, patent/licensing arrangements, etc) that might pose a conflict of interest in connection with the submitted article.

All ICMJE Conflict of Interest Forms for authors and *Clinical Orthopaedics and Related Research* editors and board members are on file with the publication and can be viewed on request. Each author certifies that his or her institution approved the reporting of this case report, that all investigations were conducted in conformity with ethical principles of research, and that informed consent for participation in the study was obtained. This work was performed at Mount Sinai Medical Center.

Y. Epelboym
Mount Sinai School of Medicine, New York, NY, USA

K. R. Desai
Greenwich Radiology Group, Greenwich
Hospital, Greenwich, CT, USA

R. Garcia
Department of Pathology, Mount Sinai
Medical Center, New York, NY, USA

J. C. Wittig (✉)
Department of Orthopedic Surgery, Mount Sinai Medical Center,
New York, NY, USA
e-mail: drjameswittig@aol.com; james.wittig@mountsinai.org

J. C. Wittig
Hackensack University Medical Center, Hackensack, NJ, USA

was significant for a father who had an unspecified sarcoma of the leg. Physical examination showed full ROM in the extremities, with no lymphadenopathy, palpable masses, or reproducible tenderness. Complete blood count, chemistries, and erythrocyte sedimentation rate were normal whereas her C-reactive protein was slightly elevated at 5.3 mg/L (reference, 0–4.9 mg/L).

The patient underwent plain radiography (Fig. 1), CT (Fig. 2), MRI (Fig. 3), and bone scintigraphy (Fig. 4).

Based on the history, physical examination, laboratory studies, and imaging studies, what is the differential diagnosis at this point?

Imaging Interpretation

Plain radiographs showed a mixed hyperdense-lytic endosteal-based lesion in the lateral supracondylar femur (Fig. 1). No periosteal reaction, cortical destruction, or extraosseous soft tissue mass was identified.

The CT scans showed a lytic lesion in the lateral supracondylar femur with a thick dense border and additional surrounding sclerosis. Axial (Fig. 2A) and coronal (Fig. 2B) reformatted CT images showed the lytic lesion in the lateral supracondylar femur with surrounding sclerosis. There was no internal mineralization or trabeculation. There was no periosteal reaction, cortical destruction, or extraosseous soft tissue mass.

Subsequent MRI showed a well-defined T1 hypointense, T2 hyperintense mass with a surrounding border of T1 hypointensity, which corresponded to the dense margins observed on the CT scans. A coronal T1-weighted image showed a T1 hypointense mass in the femur with a more hypointense border corresponding to the sclerosis observed on CT (Fig. 3A). Small amounts of surrounding marrow

Fig. 1A–B (A) PA and (B) lateral radiographs show a mixed hyperdense-lytic lesion in the lateral supracondylar femur without periosteal reaction, cortical destruction, or extraosseous soft tissue mass.

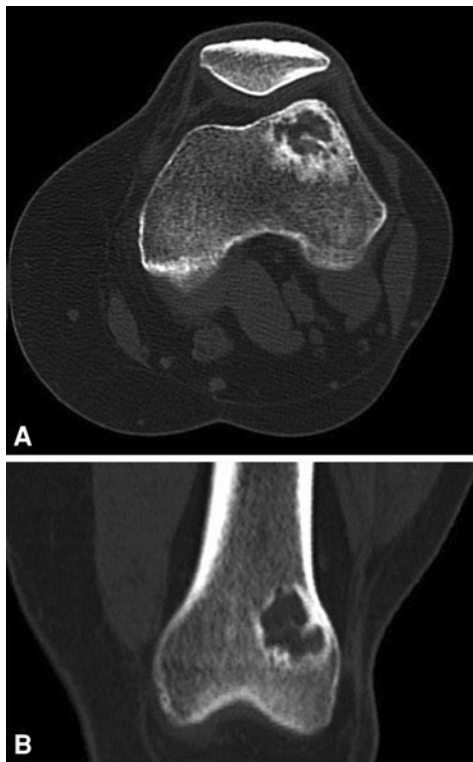
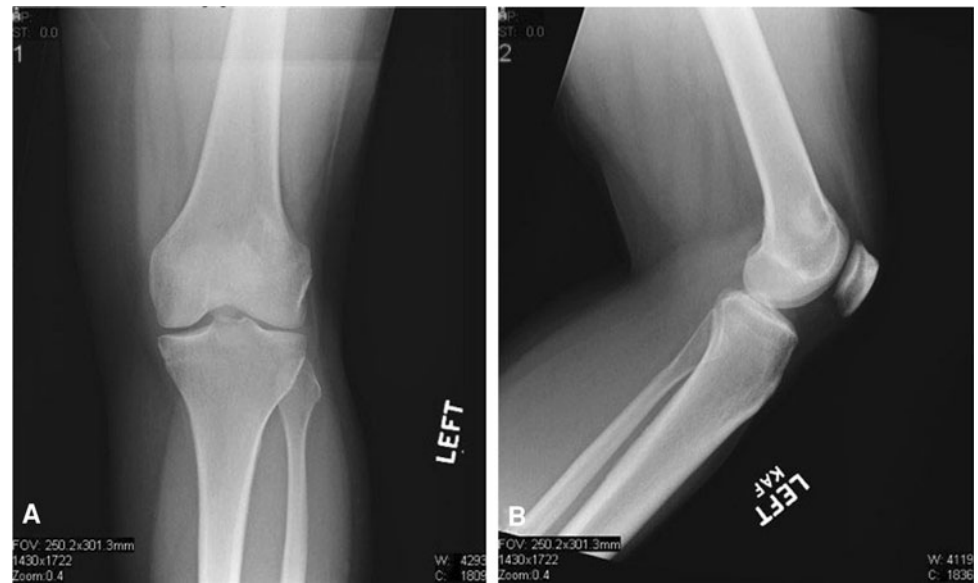


Fig. 2A–B (A) Axial and (B) coronally reformatted CT scans show a lytic lesion in the lateral supracondylar femur with surrounding sclerosis. No definite osseous or cartilaginous matrix was seen.

T1 hypointensity and T2 hyperintensity were present. No cortical destruction or extraosseous soft tissue mass was identified. An axial T2-weighted fat-saturated image showed a predominantly T2 hyperintense lesion in the lateral supracondylar femur (Fig. 3B). The lesion had intense radiotracer uptake on bone scintigraphy (Fig. 4). There were no other abnormal areas of uptake.

Differential Diagnosis

- Langerhans cell histiocytosis
- Osteoblastoma
- Aneurysmal bone cyst – solid variant
- Brodie’s abscess
- Fibrosarcoma
- Fibrous dysplasia
- Low-grade intraosseous osteosarcoma

We performed an open biopsy and analyzed histologic samples (Fig. 5).

Based on the history, physical examination, laboratory studies, imaging studies, and histologic picture, what is the diagnosis and how should this lesion be treated?

Histology Interpretation

The open biopsy (curettage) specimen consists of a $2.5 \times 2.0 \times 0.5$ cm aggregate of tan-pink friable tissue and a $0.8 \times 0.7 \times 0.5$ cm irregular portion of tan-white bone. The resection specimen consists of an oblong fragment of tan, hard bone measuring $4.0 \times 2.5 \times 2.5$ cm, with a 1.7×1.5 cm central cavity filled with cement. Microscopically, the tumor is composed of moderately cellular fibrous tissue and irregular trabeculae of woven bone. The tumor cells are predominantly spindled and frequently show large hyperchromatic nuclei and mild to moderate pleomorphism (Fig. 5A). The tumor cells are closely associated to woven bone trabeculae (Fig. 5A–B). There are two to three mitoses in 10 high power fields in the most proliferative areas. No atypical forms are seen. Necrosis is absent. The tumor has a permeative growth pattern infiltrating the intertrabecular spaces and entrapping preexisting lamellar

Fig. 3A–B (A) A coronal T1-weighted MR image shows a T1 hypointense mass in the femur with a more hypointense border corresponding to the sclerosis observed on the CT. (B) An axial T2-weighted fat-saturated MR image shows a predominantly T2 hyperintense lesion in the lateral supracondylar femur with a small amount of surrounding bone marrow edema.

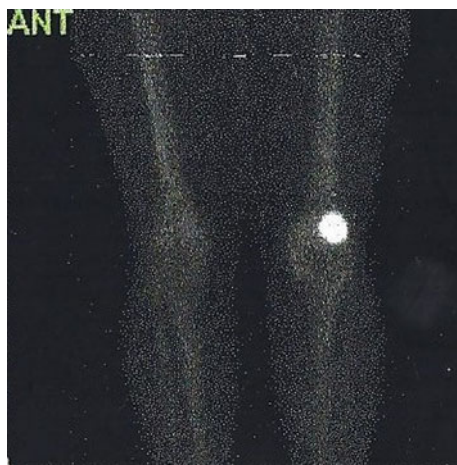
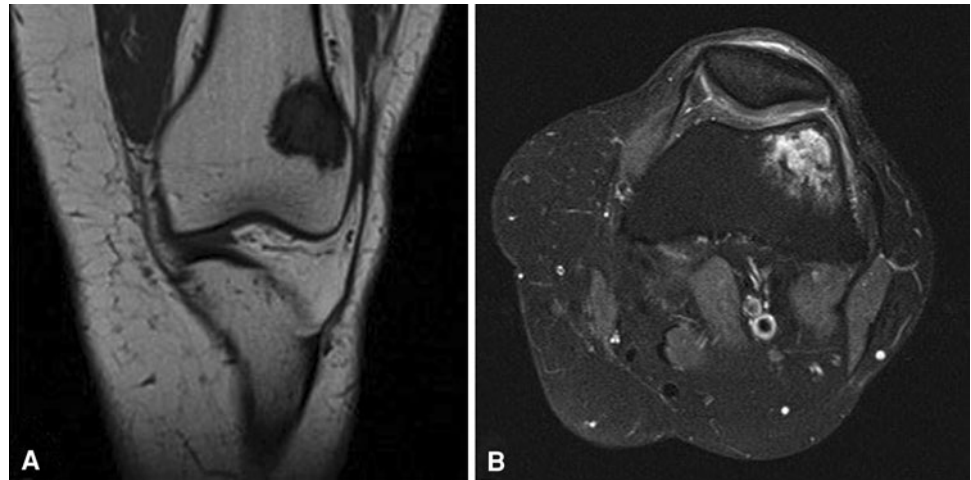


Fig. 4 An anterior-view bone scintigram shows increased radiotracer uptake in the left lateral supracondylar femur.

bone (Fig. 5C–D). This feature is seen in the curettage specimen and at the periphery of the biopsy cavity in the resection specimen (Fig. 5E).

Diagnosis

Low-grade intraosseous osteosarcoma.

Discussion and Treatment

Despite the benign appearance on plain radiography, the diagnosis of low-grade intraosseous osteosarcoma was based on histologic appearance and observation of a permeative growth pattern of the tumor. On imaging, the lesion exhibited well-defined and well-demarcated boundaries with a narrow zone of transition suggesting a slow-growing lesion. The lesion was not associated with

periosteal reaction, cortical destruction or extraosseous extension to suggest aggressive behavior. Kurt et al. [12] found an intraosseous osteosarcoma had a highly variable radiographic appearance, which at times was deceptively benign [12]. In contrast, the imaging appearance of a conventional osteosarcoma has been well established with plain radiography being the key imaging modality for its diagnosis [19]. Low-grade intraosseous osteosarcomas are slow growing; therefore their radiographic appearance is distinct from that of conventional osteosarcomas, which tend to have ill-defined borders with a wide zone of transition, attendant periosteal reaction, and cortical destruction [17]. The periosteal reaction of a conventional osteosarcoma can present as a Codman's triangle or with more of a sunburst appearance. A series of 80 cases of low-grade osteosarcoma found periosteal new bone formation present in 16 (22%) of these tumors [12]. Trabeculation, which sometimes was bizarre and often pronounced, was common and seen in 46 (62%) of these lesions [12]. MRI has assumed an invaluable role in characterizing extraosseous soft tissue extension of the tumor, defining the borders of the tumor, demarcating extent of perilesional edema, and searching for skip metastases [19, 21].

Langerhans cell histiocytosis (LCH) predominantly affects children, adolescents, and young adults and can occur in any bone [9]. Patients typically are asymptomatic. The diagnosis usually is based on radiographic evidence of a destructive bone lesion arising from the marrow cavity and on characteristic morphologic findings [9]. These findings include an expanding erosive accumulation of histiocytes, usually in the medullary cavity [9]. On microscopy, proliferation of foamy and vacuolated histiocytes is associated with a mixture of neutrophils, eosinophils, lymphocytes, and plasma cells [9]. Osteoblastoma affects males more often than females with a respective ratio of 2:1 [20]. The predilection of osteoblastoma is to affect the spine. It also can affect the long bones in the epiphysis, metaphysis, and

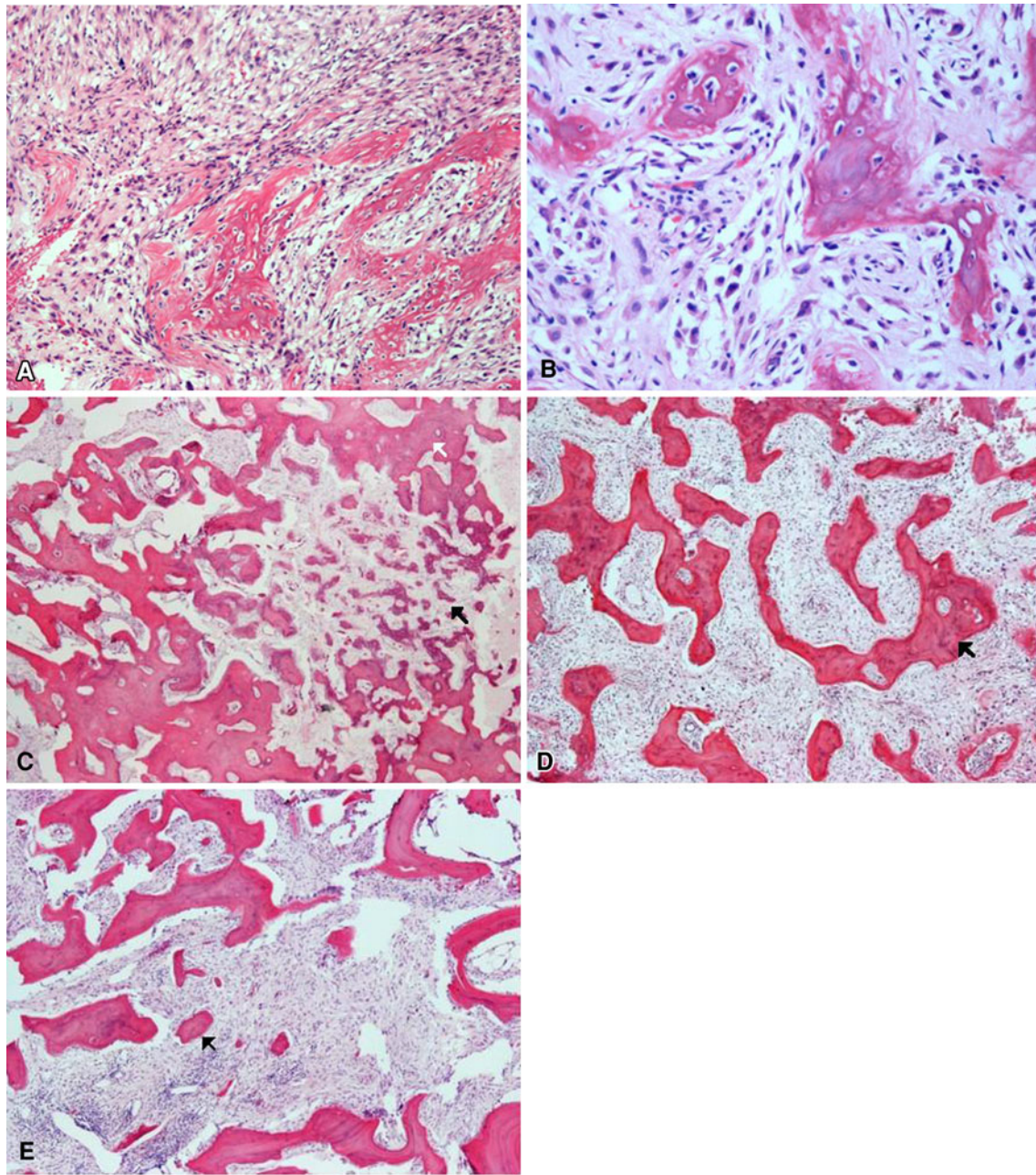


Fig. 5A–E (A) A tumor section shows moderately cellular fibrous tissue with irregular woven bone trabeculae, nuclear atypia, and moderate pleomorphism (Stain, hematoxylin & eosin; original magnification, $\times 10$). (B) At higher magnification, atypical spindle to polygonal cells with hyperchromatic nuclei closely associated with the irregular woven bone trabeculae can be seen (Stain, hematoxylin & eosin; original magnification, $\times 20$). (C) A low-power view of the curettage specimen is shown. The tumor infiltrates the intertrabecular spaces with small and irregular woven bone trabeculae (black arrow)

juxtaposed to the preexisting lamellar bone (white arrow) (Stain, hematoxylin & eosin; original magnification, $\times 2$). (D) A curettage specimen with tumor shows a permeative growth pattern with moderately cellular tumor infiltrating the intertrabecular spaces and entrapping lamellar bone (arrow) (Stain, hematoxylin & eosin; original magnification, $\times 4$). (E) In the resection specimen there is tumor infiltration of the intertrabecular spaces at the periphery of the biopsy cavity with entrapment of bone trabeculae (arrow) (Stain, hematoxylin & eosin; original magnification, $\times 4$).

diaphysis. A common complaint is of progressive pain localized at the tumor site [20]. Radiographic studies typically do not show matrix mineralization; however, CT scans may delineate the presence of mineralization and aid in diagnosis [20]. Pathologic examination of osteoblastoma

usually reveals a well-circumscribed dense border with associated surrounding edema. Osteoblast cells are often pleomorphic and plump and can have nuclei that vary from large to small with abundant cytoplasm [20]. The term aneurysmal refers to a blowout distention, and cyst refers to

the common presence of a blood-filled cavity [2, 5, 14]. The cells that line the aneurysmal bone cyst wall are composed of fibrous components and giant cells [14]. Sanerkin et al. described a solid variant of aneurysmal bone cysts in which the predominant histologic feature was that of the solid reactive material of a cystic aneurysmal bone cyst [18]. Histologically these lesions may be mistaken for low-grade osteosarcoma [1, 15]. Solid aneurysmal bone cysts have a varied radiographic appearance, occur more frequently on the metaphyseal and diaphyseal portions of long bones, and on MR images show solid and cystic elements in an expansive osteolytic lesion [8]. Brodie's abscess is one type of subacute osteomyelitis. Subacute osteomyelitis commonly affects individuals from 2 to 15 years old but reportedly affects individuals into their fourth decade of life [10]. The lower limb is affected much more frequently than the upper limb, and the tibia is affected relatively more often than the femur [10]. Brodie's abscess is typically well circumscribed with a dense border, cortical thickening, and edema and has nonspecific findings on bone scintigraphy [10]. MRI can support the diagnosis of Brodie's abscess by way of the penumbra sign, which was reported by Grey et al. [6] to have 75% sensitivity and 99% accuracy in subacute osteomyelitis. The penumbra sign is a discrete transition zone of hyperintense signal between the intermediate- to low-signal-intensity abscess cavity and the adjacent edematous or hyperdense bone marrow on T1 imaging [6]. Fibrosarcoma of bone peaks in the fourth decade and typically affects similar skeletal sites as osteosarcoma [16]. Fibrosarcoma is a painful lesion, typically appears osteolytic on radiography, and may lead to pathologic fracture. Pathologic examination shows a varying amount of fibroblast-like cells with spindle-shaped nuclei [13]. Low-grade fibrosarcomas form a large amount of collagen fiber resembling a desmoplastic fibroma [16]. In contrast high-grade fibrosarcomas have a higher mitotic index and less collagen fiber formation [16]. High-grade fibrosarcomas have a poorer prognosis as compared with low-grade fibrosarcomas [16]. Fibrous dysplasia is a benign process believed to be caused by failure of remodeling of primitive bone into lamellar bone [4]. Lesions may be monostotic or polyostotic and occur in greatest frequency in the long bones, ribs, and craniofacial bones [4]. Polyostotic lesions are less common than monostotic lesions, and frequently grow after skeletal maturity is achieved [7]. Monostotic lesions are typically asymptomatic and often are identified incidentally. On radiography, the lesion is bound by a distinct rim of reactive bone, is more radiolucent than normal bone, and has a ground-glass pattern with no appreciable trabecular pattern [4]. Histologically, fibrous dysplasia appears as immature bone lacking osteoblastic rimming in a fibrous stroma of dysplastic spindle-shaped cells lacking any cellular characteristics of malignancy [4].

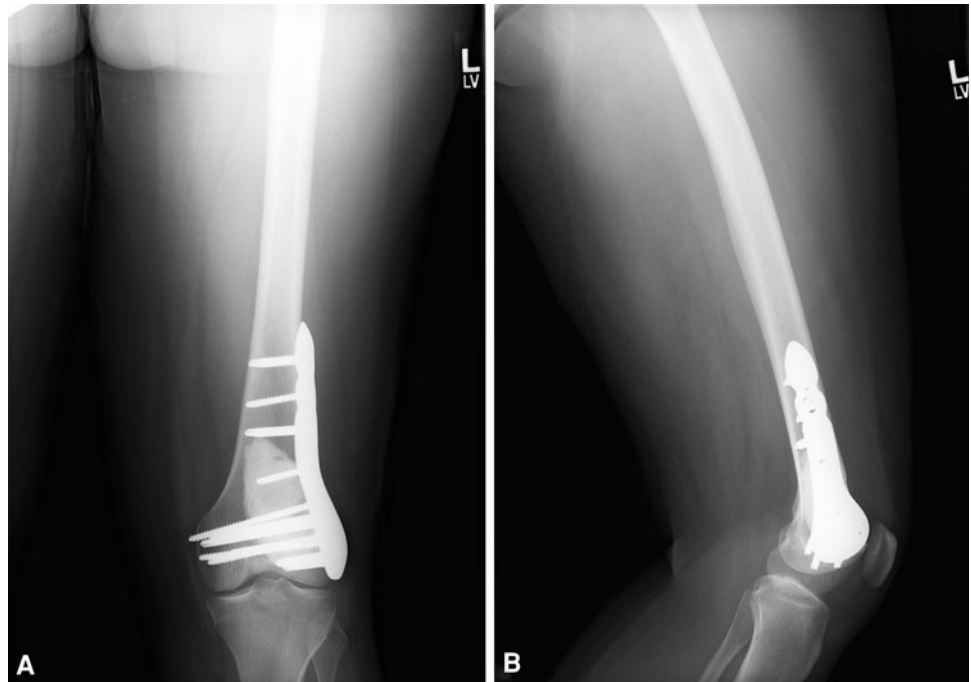
Low-grade intraosseous osteosarcoma is a rare tumor and represents 1.9% of all osteosarcomas according to a Mayo Clinic series of 4074 cases [11]. The most common symptom of low-grade osteosarcoma is pain in the associated region [2, 11, 12] and in some cases swelling. Low-grade osteosarcoma is difficult to diagnose because of variable and atypical radiographic findings and pathologic findings suggestive of benign fibrous lesions [11, 12]. Kurt et al. [12] reported on 80 cases of low-grade intraosseous osteosarcomas in 41 males and 39 females. Presentation typically occurred between the second and fifth decades of life, and the tumor had a predilection for the long bones, with a majority of the tumors developing in the femur (54%) and tibia (21%) [12].

On gross examination, low-grade intraosseous osteosarcomas are firm and fibrous with typically well-demarcated borders. Microscopically, they consist of a spindle cell tumor with irregular woven bone production, low cellularity, and few mitotic figures [12]. Various histologic patterns have been observed, with a common theme of low mitotic rates, irregular calcified osteoid, and scattered seams of osteoid embedded in collagen stroma [12]. The amount of osteoid with the tumors is variable, with some showing only small foci of osteoid [12]. Benign fibroosseous lesions of bone such as fibrous dysplasia histologically appear similar to low-grade osteosarcoma. At first glance, both consist of fibrous tissue with scattered irregular trabeculae of woven bone. Cellularity and atypia are more pronounced in low-grade osteosarcomas and mitotic figures are usually present. The expertise of an experienced pathologist often is required to distinguish these two lesions. In addition, careful correlation with the radiographic findings is extremely important.

Treatment for a low-grade intraosseous osteosarcoma typically entails en bloc resection and rarely amputation. As it is a low-grade tumor, chemotherapy and radiation typically are not used in treatment. Disease recurrence after curettage or marginal excision is 80% to 100%; in contrast, recurrence after wide resection is less than 5% [3]. This tumor is associated with a low rate of systemic metastases. The 5- and 10-year survival rates are 90% and 85%, respectively [3]. In the population of tumors that recur, 15% are high-grade osteosarcomas and the prognosis is similar to that of conventional osteosarcomas [3]. Kurt et al. [12] reported 15% of patients experienced a transformation from a low-grade osteosarcoma to a high-grade tumor. In these patients, the clinical course was similar to that of other patients with high-grade osteosarcomas. In the tumors that recurred, dedifferentiation of low-grade osteosarcoma was not an uncommon phenomenon.

We treated our patient with an en bloc resection and open reduction and internal fixation with cement. At 19 months followup she had no pain or swelling.

Fig. 6A–B (A) PA and (B) lateral radiographs of the femur show hardware in good position and no recurrence of the tumor.



On physical examination, she had good ROM. Followup radiographs showed no lesions in the femur and proper positioning of hardware (Fig. 6).

Acknowledgment We thank Camilo E. Villalobos MD for support in preparation of this manuscript.

References

- Bertoni F, Bacchini P, Capanna R, Ruggieri P, Biagini R, Ferruzzi A, Bettelli G, Picci P, Campanacci M. Solid variant of aneurysmal bone cyst. *Cancer*.1993;71:729–734.
- Campanacci M. Aneurysmal bone cyst. In: Campanacci M, ed. *Bone and Soft Tissue Tumors*. 2nd ed. New York, NY: Springer Verlag; 1999:812–840.
- Dedmond B, Eady J. Low-grade central osteosarcoma. *eMedicine*. WebMD, March 10, 2009. Available at: <http://emedicine.medscape.com/article/1255939-overview>. Accessed December 20, 2009.
- DiCaprio MR, Enneking WF. Fibrous dysplasia: pathophysiology, evaluation, and treatment. *J Bone Joint Surg Am*. 2005;87:1848–1864.
- Freiberg AA, Loder RT, Heidelberger KP, Heisinger RN. Aneurysmal bone cysts in young children. *J Pediatr Orthop*. 1994; 14:86–91.
- Grey AC, Davies AM, Mangham DC, Grimer RJ, Ritchie DA. The “penumbra sign” on T1 weighted MR imaging in subacute osteomyelitis: frequency, cause and significance. *Clin Radiol*. 1998;53:587–592.
- Henry A. Monostotic fibrous dysplasia. *J Bone Joint Surg Br*.1969; 51:300–306.
- Ilaslan H, Sundaram M, Unni KK. Solid variant of aneurysmal bone cysts in long tubular bones. *AJR Am J Roentgenol*. 2003; 180:1681–1687.
- Khan AN, Chandramohan M, Turnbull I, Macdonald S. Eosinophilic granuloma, skeletal. *eMedicine*. WebMD, May 14, 2008. Available at: <http://emedicine.medscape.com/article/389350-overview#a19>. Accessed December 20, 2009.
- Khoshhal K, Letts RM. Subacute osteomyelitis (Brodie abscess). *eMedicine*. WebMD, July 18, 2008. Available at: <http://emedicine.medscape.com/article/1248682-overview>. Accessed December 20, 2009.
- Krishnan KU, Dahlin DC, McLeod RA, Pritchard DJ. Intraosseous well-differentiated osteosarcoma. *Cancer*. 1977;40:1337–1347.
- Kurt AM, Krishnan KU, McLeod RA, Pritchard DJ. Low grade intraosseous osteosarcoma. *Cancer*. 1990;65:1418–1428.
- Larsson SE, Lorentzon R, Boquist L. Fibrosarcoma of bone: a demographic, clinical, and histopathological study of all cases recorded in the Swedish Cancer Registry from 1958 to 1968. *J Bone Joint Surg Br*. 1976;58:412–417.
- Mankin HJ, Hornicek FJ, Ortiz-Cruz E, Villafuerte J, Gebhardt MC. Aneurysmal bone cyst: a review of 150 patients. *J Clin Oncol*. 2005;23:6756–6762.
- Mirra JM, Pecci P, Gold RH, eds. *Bone Tumors: Clinical, Radiologic, and Pathologic Correlations*. Philadelphia, PA: Lea & Febiger; 1989:1267–1311.
- Randall RL, Hoang BH. Musculoskeletal oncology. In: Skinner HB, ed. *Current Diagnosis & Treatment in Orthopedics*. 4th ed. New York, NY: McGraw-Hill; 2006: 298–380. Available at: <http://www.accessmedicine.com/content.aspx?aID=2320059>. Accessed December 17, 2011.
- Resnick D. *Bone and Joint Imaging*. 2nd ed. Philadelphia, PA: WB Saunders Co; 1996.
- Sanerkin NG, Mott MG, Roylance J. An unusual intraosseous lesion with fibroblastic, osteoclastic, osteoblastic, aneurysmal and fibromyxoid elements: “solid” variant of aneurysmal bone cyst. *Cancer*. 1983;51:2278–2286.
- Seeger LL, Gold RH, Chandnani, VP. Diagnostic imaging of osteosarcoma. *Clin Orthop Relat Res*. 1991;270:254–263.
- Villalobos CE, Rybak LD, Steiner GC, Wittig JC. Osteoblastoma of the sternum. *Bull NYU Hosp Joint Dis*. 2010;68:55–59.
- Zimmer WD, Berquist TH, McLeod RA, Sim FH, Pritchard DJ, Shives TC, Wold LE, May GR. Magnetic resonance imaging of osteosarcomas: comparison with computed tomography. *Clin Orthop Relat Res*. 1986;208:289–299.